

Radicals | Hot Paper |

Quinoidal Oligo(9,10-anthryl)s with Chain-Length-Dependent Ground States: A Balance between Aromatic Stabilization and Steric Strain Release

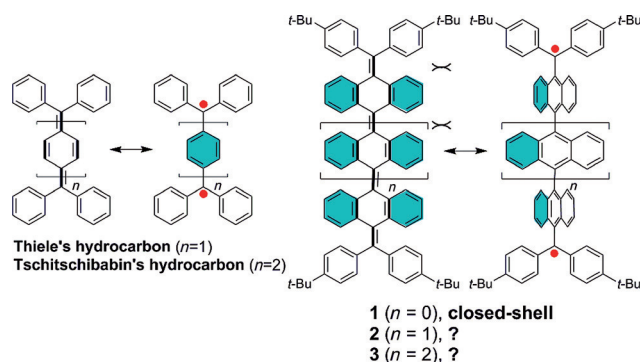
Zhenglong Lim,^[a] Bin Zheng,^[b] Kuo-Wei Huang,^{*[b]} Ye Liu,^{*[c]} and Jishan Wu^{*[a, c]}

Abstract: Quinoidal π -conjugated polycyclic hydrocarbons have attracted intensive research interest due to their unique optical/electronic properties and possible magnetic activity, which arises from a thermally excited triplet state. However, there is still lack of fundamental understanding on the factors that determine the electronic ground states. Herein, by using quinoidal oligo(9,10-anthryl)s, it is demonstrated that both aromatic stabilisation and steric strain release play balanced roles in determining the ground states. Oligomers with up to four anthryl units were synthesised and their ground states were investigated by electronic absorption and electron spin resonance (ESR) spectroscopy, assisted by density functional theory (DFT) calculations. The

quinoidal 9,10-anthryl dimer **1** has a closed-shell ground state, whereas the tri- (**2**) and tetramers (**3**) both have an open-shell diradical ground state with a small singlet–triplet gap. Such a difference results from competition between two driving forces: the large steric repulsion between the anthryl/phenyl units in the closed-shell quinoidal form that drives the molecule to a flexible open-shell diradical structure, and aromatic stabilisation due to the gain of more aromatic sextet rings in the closed-shell form, which drives the molecule towards a contorted quinoidal structure. The ground states of these oligomers thus depend on the overall balance between these two driving forces and show chain-length dependence.

Introduction

Polycyclic aromatic hydrocarbons (PAHs) have, over the past few decades, garnered increasing interest, especially in the field of organic materials science and structural organic chemistry.^[1] Although most PAHs exist in the closed-shell electronic configuration, recent research has revealed that certain types of quinoidal polycyclic hydrocarbons (PHs) could show an open-shell singlet diradical ground state and display unique optical, electronic and magnetic properties.^[2] These quinoidal PHs can be regarded as pro-aromatic systems due to the recovery of one or more aromatic sextet rings (highlighted in blue in Scheme 1) in the open-shell diradical form, and typical examples are the Thiele hydrocarbon^[3] and the Tschitschibabin



Scheme 1. Resonance structures of the Thiele hydrocarbon, the Tschitschibabin hydrocarbon, and the quinoidal oligo(9,10-anthryl)s 1–3.

[a] Z. Lim, Prof. J. Wu
Department of Chemistry, National University of Singapore
3 Science Drive 3, 117543 (Singapore)
Fax: (+65) 6779-1691
E-mail: chmwuj@nus.edu.sg

[b] Dr. B. Zheng, Prof. K.-W. Huang
Division of Physical Sciences & Engineering and
KAUST Catalysis Center, King Abdullah University of
Science and Technology (KAUST), Thuwal 23955-6900, (Saudi Arabia)
E-mail: kuowei.huang@kaust.edu.sa

[c] Dr. Y. Liu, Prof. J. Wu
Synthesis & Integration, Institute of Materials Research
and Engineering, 3 Research Link, 117602 (Singapore)
E-mail: ye-liu@imre.a-star.edu.sg

Supporting information for this article is available on the WWW under
<http://dx.doi.org/10.1002/chem.201503033>.

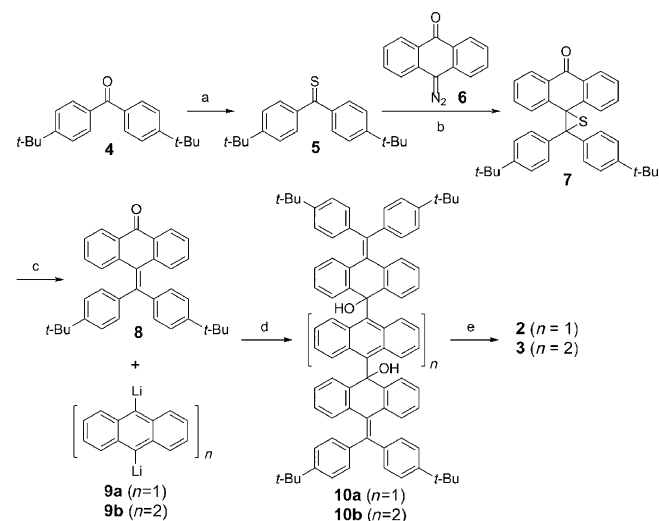
hydrocarbon,^[4] which were first prepared more than 100 years ago and many recent studies are inspired therefrom. Whereas the Thiele hydrocarbon is sufficiently stable, the Tschitschibabin hydrocarbon is highly reactive and can only be isolated in an inert atmosphere.^[5] The instability of the latter comes from its large diradical character because two more aromatic sextets are generated from the closed-shell quinoidal form to the open-shell diradical form. Thus, the synthesis of more extended quinoidal PHs is a big challenge. One way is to embed pro-aromatic *p*-quinodimethane (*p*-QDM), 2,6-naphthoquinodimethane or 2,6-anthraquinodimethane moieties into a π -conjugated PAH framework to form relatively stable quinoidal PHs. Examples of this type include bis(phenalenyl)s,^[6] zethrenes^[7]

and indenofluorenes,^[8] and many of them display very interesting open-shell singlet diradical characteristics in the ground state. Another approach is to stabilise the extended *p*-QDMs by benzannulation, for example, very stable tetrabenzot-schibabin hydrocarbon **1**^[9] (Scheme 1) was successfully synthesised by us, and this concept has been successfully extended to a series of quinoidal rylene based diradicaloids.^[10] Molecule **1** has a closed-shell ground state with a butterfly geometry in the single crystals to minimise steric repulsion between the anthryl/phenyl units, and it is believed that aromatic stabilisation by two more aromatic sextet rings in the closed-shell form is the origin of a contorted quinoidal structure rather than a flexible open-shell diradical form. It seems that a balance between aromatic stabilisation and steric repulsion plays a critical role in determining the ground state. This raises the question of the ground state of the more extended analogues, quinoidal 9,10-anthryl trimer **2** and tetramer **3** (Scheme 1). With extension of the chain length, both driving forces are enforced and it is interesting to determine the changes to the ground states and physical properties with increasing chain length. In this context, herein, we report the synthesis of quinoidal oligo(9,10-anthryl)s **2** and **3**, and detailed studies on their ground states, physical properties and chemical reactivity. Insights from this study would enhance our understanding of the reaction mechanisms involved in the synthesis of atomically precise graphene nanoribbons.^[11] Our studies demonstrate that a balance between aromatic stabilisation and steric strain release finally determine the ground states of these oligomers.

Results and Discussion

Synthesis, optical properties and stability

The synthetic route to **2** and **3** is shown in Scheme 2. Key intermediates are diols **10a/10b**. Treatment of 4,4'-di-*tert*-butyl-



Scheme 2. Synthetic routes to **2** and **3**. Reaction conditions: a) Lawesson's reagent, toluene, 80 °C, overnight; b) THF, RT, overnight; c) PPh₃, toluene, 24 h, 89% yield over three steps; d) THF, -78 °C, 1 h, 12–13% yield; e) SnCl₂, CH₂Cl₂, quantitative yield.

benzophenone (**4**)^[12] with Lawesson's reagent gave the thioether **5**, which reacted with the 10-diazo-9-anthrone (**6**)^[12] to generate the thioepoxide **7**. Reaction of **7** with PPh₃ afforded the desired ketone **8** in 89% yield over three steps. The 9,10-dibromoanthracene and 10,10'-dibromo-9,9'-bianthryl^[13] compounds were separately lithiated with *n*BuLi to give intermediates **9a/9b**, which reacted with ketone **8** to afford precursors diols **10a/10b** in 12 and 13% yield, respectively.

Subsequent reduction of **10a/10b** with SnCl₂ in CH₂Cl₂ under an inert atmosphere gave target compounds **2** and **3** in nearly quantitative conversion (based on MS and TLC analysis). However, both products were unstable on silica gel or aluminium oxide columns and thus they were isolated simply by filtration of the resulting solution through a 0.45 μm polytetrafluoroethylene (PTFE) syringe cartridge followed by removal of the solvent under vacuum.

The MALDI-TOF mass spectra of **2** and **3** both agree well with their respective molecular weights, with loss of two hydroxyl groups (see the Supporting Information). The absorption spectra of freshly synthesised **2** and **3** are shown in Figure 1. Both compounds display two sharp bands (**2**: λ = 499 and 533 nm, **3**: λ = 500 and 533 nm) and a broad absorption band between λ = 650 and 1050 nm, with bands at λ ≈ 813 and 801 nm, respectively. The long-wavelength broad absorption bands are very similar to the in situ generated diradical of dimer **1**,^[9] which indicates that both **2** and **3** are open-shell di-

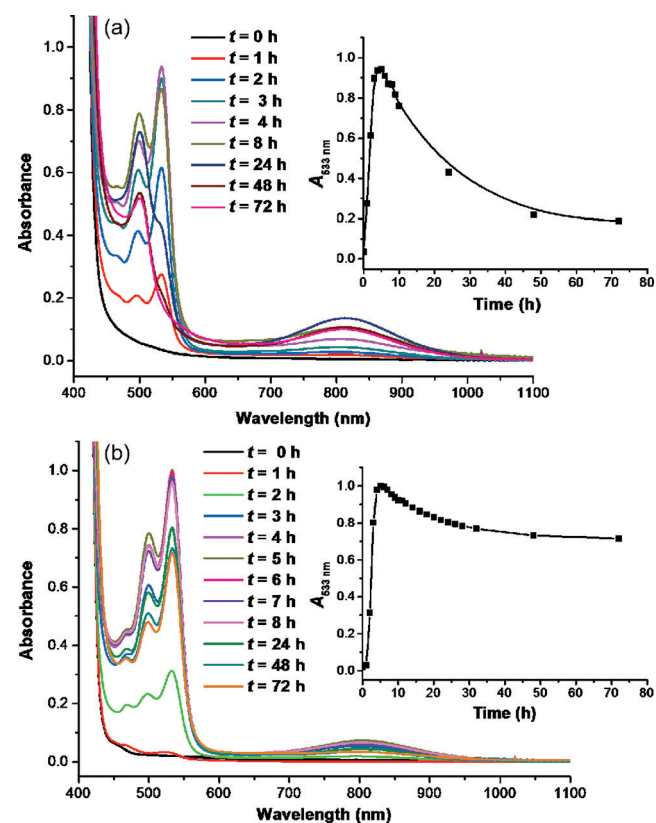


Figure 1. UV/Vis/near-infrared (NIR) absorption spectra of in situ generation of a) **2** and b) **3** in dry toluene from their precursors, **10a** and **10b** respectively (*t* = 0 h). Insets: plots showing the changes of the absorbance at λ = 533 nm with time.

radicals rather than a closed-shell quinoidal compound. A small optical energy gap of about 1.23 eV was estimated for both compounds. Strong electron spin resonance (ESR) signals showing hyperfine coupling were detected for the freshly prepared samples in CH_2Cl_2 (below), which suggested the paramagnetic character of both **2** and **3**.

UV/Vis/NIR absorption spectroscopic measurements were used to follow the generation and decay processes of **2** and **3** in dry toluene under a nitrogen atmosphere (Figure 1). Both **2** and **3** show similar absorption patterns to that of compound **1**^[9] (sharp band at $\lambda=507$ nm and a broad absorption band between $\lambda=680$ and 1050 nm) in the open-shell electronic conformation, which indicates that these compounds undergo formation of a biradical electronic state before decomposition proceeds. The plot of absorbance (at $\lambda=533$ nm for both **2** and **3**) versus time revealed that the initial generation of **2** and **3** reached a maximum in about 4 h and then gradually decayed over a span of days. The ESR signals of the freshly prepared samples showed similar degradation over time, and the colour of the sample solutions gradually changed from red to yellowish brown in one week, even when placed under an argon atmosphere throughout. The slow decay is believed to be due to some intermolecular radical–radical coupling reactions and reaction with residual oxygen in the solution. Gel permeation chromatography (GPC) measurements were performed on the fresh and one-week-old samples of both **2** and **3** (Figures S1–S4 in the Supporting Information) and a new low-intensity broad band was observed in the high-molecular-weight region after one week of storage, which suggested the formation of oligo- or polymers in both cases. The ^{13}C NMR spectra of **2** and **3** after storage for one week revealed the appearance of signals for a carbonyl group ($\delta=156.02$ and 168.14 ppm for compounds **2** and **3**, respectively; Figures S7 and S8 in the Supporting Information), as further supported by FTIR measurements. New vibrational bands at $\tilde{\nu}=1671$ and 1658 cm^{-1} correlated to $\nu_{\text{C=O}}$ were observed (Figure S14 and S15 in the Supporting Information). The presence of carbonyl groups may be due to the termination of the radical sites by oxygen, which was also observed in other reactive diradicals.^[14] Nevertheless, both **2** and **3** still showed certain persistence under an inert atmosphere, which could be ascribed to steric protection of the radicals by anthryl units and spin delocalisation at the terminal units (see below).^[9,15]

Ground-state geometry and electronic structure

To understand the different ground-state electronic and geometric structures of **2** and **3** from those of **1**, broken-symmetry DFT calculations (UCAM-B3LYP/6-31G*) were performed (Figure 2). The energies of different possible geometries were calculated, and it was found that, in both cases, the triplet biradical (TB) had the lowest energy (ground state). In this form, all anthryl units are nearly orthogonal to each other and the spins are mainly delocalised along the two terminal diphenyl-anthrylmethene units (Figure 2). The two spins are nearly isolated, and thus, they are better described as two individual radicals. Accordingly, a small singlet–triplet energy gap of

2.7 kJ mol^{-1} was calculated for both **2** and **3**. The closed-shell configuration of **2** and **3** with a butterfly geometry was calculated to be 33.5 and 78.1 kJ mol^{-1} , respectively, higher in energy than the TB ground states, which indicated that the steric strain increased as the number of anthryl units increased. One more singlet diradical state for **2** and two more singlet diradical states for **3** were also calculated when mixing both the double- and single-bond linkages along the long axis, and all showed very high energies (Figure 2).

The ground-state electronic structures of **2** and **3** were further investigated by ESR measurements both in solution and in the solid state. The measured ESR signals of the freshly prepared samples of **2** and **3** in CH_2Cl_2 both showed a hyperfine structure with $g_e=2.0026$ (Figure 3a and b). The spin concentration at the peak (after reaction for 4 h), with 2,2-diphenyl-1-picrylhydrazyl (DPPH) as a standard, was determined to be about 39% for **2** and 125% for **3**, relative to the DPPH radical concentration (Figure S16 in the Supporting Information). The ESR spectrum was simulated based on the anticipated proton coupling strength obtained from calculated spin density values (Figure 3c), with the parameters $A(\text{H}1)=3.26\text{ G} (\times 4)$, $A(\text{H}2)=1.30\text{ G} (\times 2)$ and $A(\text{H}3)=1.26\text{ G} (\times 2)$ for **2** and $A(\text{H}1)=3.54\text{ G} (\times 4)$, $A(\text{H}2)=1.40\text{ G} (\times 2)$ and $A(\text{H}3)=1.40\text{ G} (\times 2)$ for **3**, both are in good agreement with the experimental data (Figure 3a and b). The solvent was removed by bubbling argon through the solution and the residual solid was submitted to temperature-dependent ESR measurements. The ESR intensity (I) increased with decreasing temperature (T), and the I versus $1/T$ curve showed a linear relationship (Figure S17 in Supporting Information), which further supporting a TB (or two isolated radicals) ground state for both. Due to the simultaneous degradation of the diradicals, the exact singlet–triplet gap was not determined.

Conclusion

We successfully synthesised quinoidal 9,10-anthryl trimer **2** and tetramer **3**, which both showed an open-shell diradical ground state and were in contrast to the closed-shell quinoidal dimer **1**. This difference could be explained by increased steric strain upon elongation of the chain length, which surpassed the aromatic stabilisation energy in the closed-shell form, and thus, led to the more flexible diradical form in the ground state. Due to the orthogonal character of the anthryl units, both **2** and **3** could be regarded as two isolated radicals, as supported by results from DFT calculations and ESR measurements. Both **2** and **3** were fairly persistent under an inert atmosphere due to kinetic blocking and spin delocalisation; however, they still underwent slow decay due to radical–radical combination and oxidation. Our research demonstrates that balancing the aromatic stabilisation and steric strain release will allow us to tune the ground state and physical properties of quinoidal PHs.

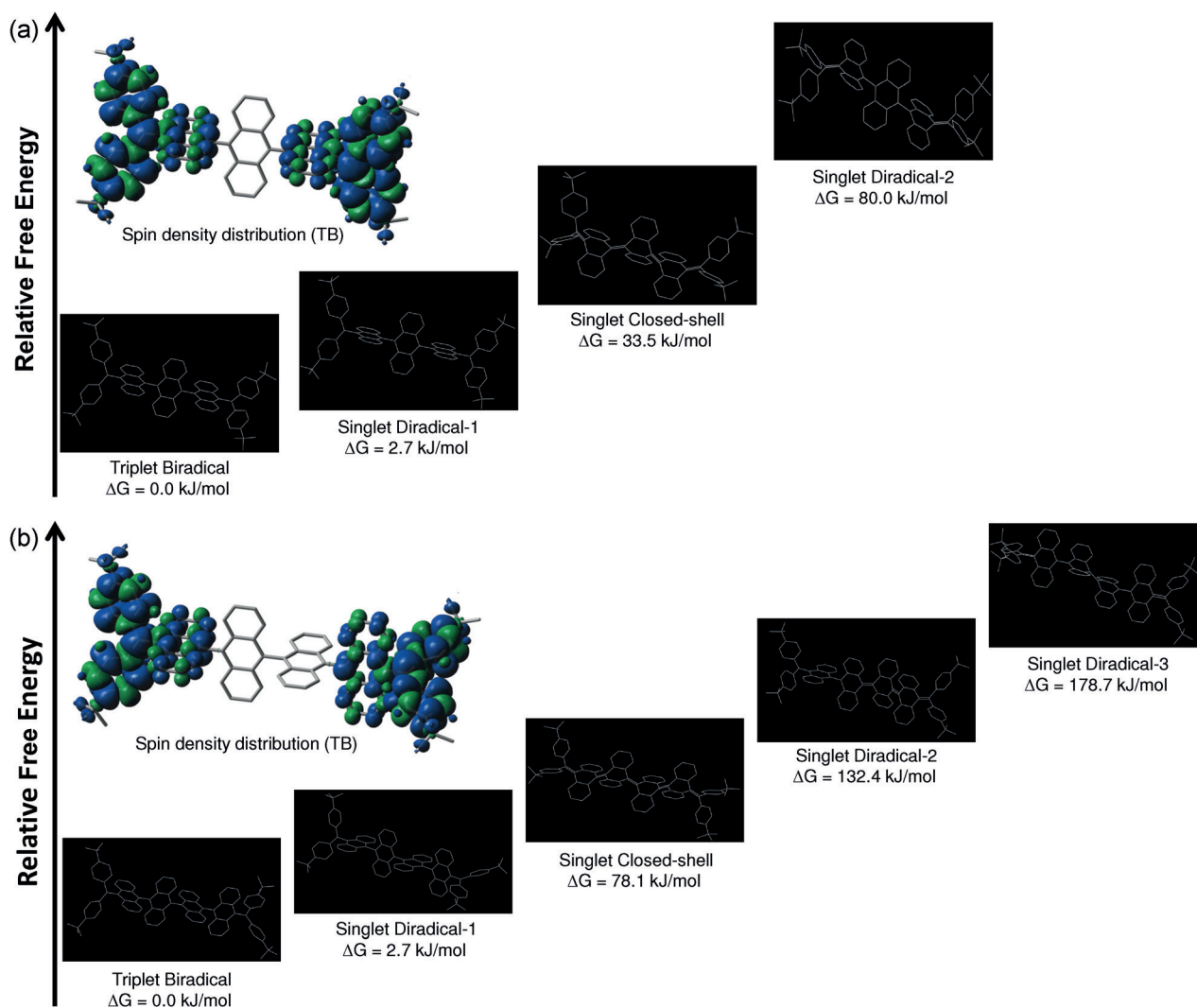


Figure 2. Calculated energies of **2** (a) and **3** (b) with different configurations. Insets: spin density distribution mappings of the triplet biradicals (TBs).

Experimental Section

Synthesis of **10a**

9,10-Dibromoanthracene (100 mg, 0.30 mmol) was added to an oven-dried Schlenk flask. The flask was then degassed and purged with argon three times before dry THF (10 mL) was added by means of a syringe. The solution was cooled to -78°C and a solution of *n*BuLi (1.6 M in hexane, 0.37 mL, 0.60 mmol) was then slowly added. The mixture was stirred for 1 h at -78°C and then a solution of **8** (294 mg, 0.62 mmol) in THF (5 mL) was added by syringe dropwise at -78°C . The solution was slowly warmed to room temperature and stirred for 3 days at RT and a clear yellow solution was obtained. Upon completion of the reaction, as monitored by TLC, the solution was quenched with water and extracted by CHCl_3 . The organic layer was washed with water and dried over anhydrous Na_2SO_4 . The solvent was removed under vacuum and the residue was purified by column chromatography (silica gel, hexane/ CH_2Cl_2 /ethyl acetate = 10/1/1, v/v/v, $R_f = 0.4$) to give a yellow solid in 12% yield. Due to the presence of isomers that could not be separated, ^1H and ^{13}C NMR spectra were not recorded. HRMS (APCI): m/z calcd for $\text{C}_{35}\text{H}_{35}\text{O}_2$: 1119.6075; found: 1119.6080.

Synthesis of **10b**

The above procedure for the synthesis was followed to prepare **10b** by using 10,10'-dibromo-9,9'-bianthryl instead of 9,10-dibromoanthracene. Compound **10b** was obtained as a yellow solid in 13% yield. HRMS (APCI): m/z calcd for $\text{C}_{98}\text{H}_{87}\text{O}_2$: 1295.6701; found: 1295.6706.

Synthesis of **2** for UV measurements

In an oven-dried cuvette, anhydrous tin(II) chloride (10 mg) was added, and the cuvette was capped with a rubber septum. The cuvette was then purged with nitrogen for 15 min and a balloon of inert gas was attached to the cuvette by a syringe needle through the rubber septa. In a separate flame-dried 25 mL Schlenk tube, compound **10a** (10 mg, 8.93×10^{-6} mmol) was added. The flask was then degassed and purged with argon three times before dry toluene was added to give a yellow solution of known concentration. The resulting solution (3 mL) was then transferred to the cuvette by means of a syringe and the reaction was monitored by UV/Vis spectroscopy.

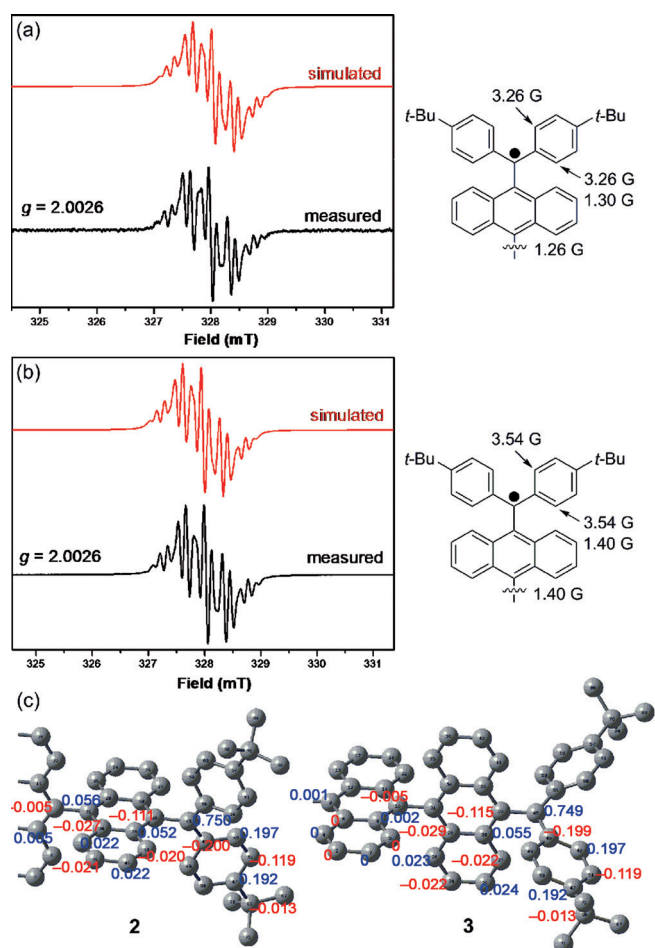


Figure 3. ESR spectra and simulated spectra of freshly prepared solutions of **2** (a) and **3** (b) in CH_2Cl_2 recorded at 193 K. c) Calculated spin densities of **2** and **3**.

Synthesis of **2** for ESR measurements

In a flame-dried 25 mL Schlenk tube, anhydrous tin(II) chloride (10 mg) was added, and the Schlenk tube was degassed and purged with argon three times. In a separate flame-dried 25 mL Schlenk tube, compound **10a** (10 mg, 8.93×10^{-6} mmol) was added. The flask was also degassed and purged with argon three times before dry dichloromethane was added to give a yellow solution. The resulting solution was then added to the Schlenk tube containing the anhydrous tin(II) chloride and the reaction was monitored by TLC. Upon completion of the reaction, the suspension was filtered through a PTFE, 25 mm diameter, 0.45 μm syringe filter. The filtered solution, when solvent was removed, gave a red-dish solid that slowly turned brown. HRMS (APCI): m/z calcd for $\text{C}_{35}\text{H}_{35}\text{O}$ [$M+1$]: 1085.6020; found: 1085.6014.

Synthesis of **3** for the respective measurements

The above procedures were followed for the preparation of **3** for analysis. Compound **3** was obtained quantitatively, as ascertained by TLC, as a red solid that slowly turned brown. HRMS (APCI): m/z calcd for $\text{C}_{35}\text{H}_{35}\text{O}$ [$M+1$]: 1261.6646; found: 1261.6631.

Acknowledgements

We acknowledge financial support from the MOE Tier 3 Programme (MOE2014-T3-1-004), Tier 2 grant (MOE2014-T2-1-080) and A*STAR JCO grant (1431AFG100). K.-W.H. thanks financial support from KAUST.

Keywords: aromaticity • electronic structure • hydrocarbons • radicals • strained molecules

- [1] a) J. Wu, W. Pisula, K. Müllen, *Chem. Rev.* **2007**, *107*, 718–747; b) *Carbon-Rich Compounds: From Molecules to Materials* (Eds.: M. M. Haley, R. R. Tykwinski), Wiley-VCH, Weinheim, **2006**; c) *Polyarenes I (Topics in Current Chemistry)*, Springer, Heidelberg, **2014**.
- [2] a) A. Rajca, *Chem. Rev.* **1994**, *94*, 871–893; b) Y. Morita, K. Suzuki, S. Sato, T. Takui, *Nat. Chem.* **2011**, *3*, 197–204; c) Z. Sun, Q. Ye, C. Chi, J. Wu, *Chem. Soc. Rev.* **2012**, *41*, 7857–7889; d) J. Casado, R. P. Ortiz, J. T. López Navarrete, *Chem. Soc. Rev.* **2012**, *41*, 5672–5686; e) A. Shimizu, Y. Hirao, T. Kubo, M. Nakano, E. Botek, B. Champagne, *AIP Conf. Proc.* **2012**, *1504*, 399–405; f) Z. Sun, Z. Zeng, J. Wu, *Chem. Asian J.* **2013**, *8*, 2894–2904; g) M. Abe, *Chem. Rev.* **2013**, *113*, 7011–7088; h) Z. Sun, Z. Zeng, J. Wu, *Acc. Chem. Res.* **2014**, *47*, 2582–2591; i) T. Kubo, *Chem. Rec.* **2015**, *15*, 218–232; j) Z. Zeng, X. Shi, C. Chi, J. T. López Navarrete, J. Casado, J. Wu, *Chem. Soc. Rev.* **2015**, *44*, 6578–6596.
- [3] J. Thiele, H. Balhorn, *Chem. Ber.* **1904**, *37*, 1463–1470.
- [4] A. E. Tschitschibabin, *Chem. Ber.* **1907**, *40*, 1810–1819.
- [5] L. K. Montgomery, J. C. Huffman, E. A. Jurczak, M. P. Grendze, *J. Am. Chem. Soc.* **1986**, *108*, 6004–6011.
- [6] a) K. Ohashi, T. Kubo, T. Masui, K. Yamamoto, K. Nakasuji, T. Takui, Y. Kai, I. Murata, *J. Am. Chem. Soc.* **1998**, *120*, 2018–2027; b) T. Kubo, M. Sakamoto, M. Akabane, Y. Fujiwara, K. Yamamoto, M. Akita, K. Inoue, T. Takui, K. Nakasuji, *Angew. Chem. Int. Ed.* **2004**, *43*, 6474–6479; *Angew. Chem.* **2004**, *116*, 6636–6641; c) T. Kubo, A. Shimizu, M. Sakamoto, M. Uruichi, K. Yakushi, M. Nakano, D. Shiomi, K. Sato, T. Takui, Y. Morita, K. Nakasuji, *Angew. Chem. Int. Ed.* **2005**, *44*, 6564–6568; *Angew. Chem.* **2005**, *117*, 6722–6726; d) A. Shimizu, M. Uruichi, K. Yakushi, H. Matsuzaki, H. Okamoto, M. Nakano, Y. Hirao, K. Matsumoto, H. Kurata, T. Kubo, *Angew. Chem. Int. Ed.* **2009**, *48*, 5482–5486; *Angew. Chem.* **2009**, *121*, 5590–5594; e) A. Shimizu, T. Kubo, M. Uruichi, K. Yakushi, M. Nakano, D. Shiomi, K. Sato, T. Takui, Y. Hirao, K. Matsumoto, H. Kurata, Y. Morita, K. Nakasuji, *J. Am. Chem. Soc.* **2010**, *132*, 14421–14428; f) A. Shimizu, Y. Hirao, K. Matsumoto, H. Kurata, T. Kubo, M. Uruichi, K. Yakushi, *Chem. Br. Chem. Commun.* **2012**, *48*, 5629–5631.
- [7] a) R. Umeda, D. Hibi, K. Miki, Y. Tobe, *Org. Lett.* **2009**, *11*, 4104–4106; b) T. C. Wu, C. H. Chem, D. Hibi, A. Shimizu, Y. Tobe, Y. T. Wu, *Angew. Chem. Int. Ed.* **2010**, *49*, 7059–7062; *Angew. Chem.* **2010**, *122*, 7213–7216; c) Z. Sun, K.-W. Huang, J. Wu, *Org. Lett.* **2010**, *12*, 4690; d) Z. Sun, K.-W. Huang, J. Wu, *J. Am. Chem. Soc.* **2011**, *133*, 11896–11899; e) Y. Li, K.-W. Heng, B. S. Lee, N. Aratani, J. L. Zafra, N. Bao, R. Lee, Y. M. Sung, Z. Sun, K.-W. Huang, R. D. Webster, J. T. López Navarrete, D. Kim, A. Osuka, J. Casado, J. Ding, J. Wu, *J. Am. Chem. Soc.* **2012**, *134*, 14913–14922; f) W. Zeng, M. Ishida, S. Lee, Y. Sung, Z. Zeng, Y. Ni, C. Chi, D.-H. Kim, J. Wu, *Chem. Eur. J.* **2013**, *19*, 16814–16824; g) Z. Sun, S. Lee, K. Park, X. Zhu, W. Zhang, B. Zheng, P. Hu, Z. Zeng, S. Das, Y. Li, C. Chi, R. Li, K. Huang, J. Ding, D. Kim, J. Wu, *J. Am. Chem. Soc.* **2013**, *135*, 18229–18236; h) Z. Sun, J. Wu, *J. Org. Chem.* **2013**, *78*, 9032–9040; i) L. Shan, Z.-X. Liang, X.-M. Xu, Q. Tang, Q. Miao, *Chem. Sci.* **2013**, *4*, 3294–3297; j) J. L. Zafra, R. C. González Cano, M. C. R. Delgado, Z. Sun, Y. Li, J. T. López Navarrete, J. Wu, J. Casado, *J. Chem. Phys.* **2014**, *140*, 054706; k) Y. Li, K.-W. Huang, Z. Sun, R. D. Webster, Z. Zeng, W. Zeng, C. Chi, K. Furukawa, J. Wu, *Chem. Sci.* **2014**, *5*, 1908–1914; l) S. Das, S. Lee, M. Son, X. Zhu, W. Zhang, B. Zheng, P. Hu, Z. Zeng, Z. Sun, W. Zeng, R.-W. Li, K.-W. Huang, J. Ding, D. Kim, J. Wu, *Chem. Eur. J.* **2014**, *20*, 11410–11420; m) Z. Sun, B. Zheng, P. Hu, K.-W. Huang, J. Wu, *ChemPlusChem* **2014**, *79*, 1549–1553; n) Z. Sun, J. Wu, *Pure Appl. Chem.* **2014**, *86*, 529–537.
- [8] a) D. T. Chase, B. D. Rose, S. P. McClintock, L. N. Zakharov, M. M. Haley, *Angew. Chem. Int. Ed.* **2011**, *50*, 1127–1130; *Angew. Chem.* **2011**, *123*, 1159–1162; b) A. Shimizu, Y. Tobe, *Angew. Chem. Int. Ed.* **2011**, *50*,

- 6906–6910; *Angew. Chem.* **2011**, *123*, 7038–7042; c) A. Fix, D. Chase, M. Haley, in *Polyarenes I*, Vol. 349 (Eds.: J. S. Siegel, Y.-T. Wu), Springer, Berlin, Heidelberg, **2014**, pp. 159–195; d) A. G. Fix, P. E. Deal, C. L. Vonnegut, B. D. Rose, L. N. Zakharov, M. M. Haley, *Org. Lett.* **2013**, *15*, 1362–1365; e) B. D. Rose, C. L. Vonnegut, L. N. Zakharov, M. M. Haley, *Org. Lett.* **2012**, *14*, 2426–2429; f) A. Shimizu, R. Kishi, M. Nakano, D. Shiomi, K. Sato, T. Takui, I. Hisaki, M. Miyata, Y. Tobe, *Angew. Chem. Int. Ed.* **2013**, *52*, 6076–6079; *Angew. Chem.* **2013**, *125*, 6192–6195; g) H. Miyoshi, S. Nobusue, A. Shimizu, I. Hisaki, M. Miyata, Y. Tobe, *Chem. Sci.* **2014**, *5*, 163–168; h) B. S. Young, D. T. Chase, J. L. Marshall, C. L. Vonnegut, L. N. Zakharov, M. M. Haley, *Chem. Sci.* **2014**, *5*, 1008–1014; i) D. Luo, S. Lee, B. Zheng, Z. Sun, W. Zeng, K.-W. Huang, K. Furukawa, D. Kim, R. D. Webster, J. Wu, *Chem. Sci.* **2014**, *5*, 4944–4952.
- [9] Z. Zeng, Y. M. Sung, N. Bao, D. Tan, R. Lee, J. L. Zafra, B. S. Lee, M. Ishida, J. Ding, J. T. López Navarrete, Y. Li, W. Zeng, D. Kim, K.-W. Huang, R. D. Webster, J. Casado, J. Wu, *J. Am. Chem. Soc.* **2012**, *134*, 14513–14525.
- [10] a) Z. Zeng, M. Ishida, J. L. Zafra, X. Zhu, Y. M. Sung, N. Bao, R. D. Webster, B. S. Lee, R.-W. Li, W. Zeng, Y. Li, C. Chi, J. T. López Navarrete, J. Ding, J. Casado, D. Kim, J. Wu, *J. Am. Chem. Soc.* **2013**, *135*, 6363–6371; b) Z. Zeng, S. Lee, J. L. Zafra, M. Ishida, X. Zhu, Z. Sun, Y. Ni, R. D. Webster, R.-W. Li, J. T. López Navarrete, C. Chi, J. Ding, J. Casado, D. Kim, J. Wu, *Angew. Chem. Int. Ed.* **2013**, *52*, 8561–8565; *Angew. Chem.* **2013**, *125*, 8723–8727; c) Z. Zeng, S. Lee, J. L. Zafra, M. Ishida, N. Bao, R. D. Webster, J. T. López Navarrete, J. Ding, J. Casado, D.-H. Kim, J. Wu, *Chem. Sci.* **2014**, *5*, 3072–3080; d) Z. Zeng, J. Wu, *Chem. Rec.* **2015**, *15*, 322–328; e) Z. Zeng, S. Lee, M. Son, K. Fukuda, P. M. Burrezo, X. Zhu, Q. Qi, R.-W. Li, J. T. López Navarrete, J. Ding, J. Casado, M. Nakano, D. Kim, J. Wu, *J. Am. Chem. Soc.* **2015**, *137*, 8572–8583.
- [11] J. Cai, P. Ruffieux, R. Jaafar, M. Bieri, T. Braun, S. Blankenburg, M. Muoth, A. P. Seitsonen, M. Saleh, X. Feng, K. Mullen, R. Fasel, *Nature* **2010**, *466*, 470–473.
- [12] X. Zhang, X. Jiang, K. Zhang, L. Mao, J. Luo, C. Chi, H. S. O. Chan, J. Wu, *J. Org. Chem.* **2010**, *75*, 8069–8077.
- [13] U. Müller, M. Baumgarten, *J. Am. Chem. Soc.* **1995**, *117*, 5840–5850.
- [14] A. Konishi, Y. Hirao, K. Matsumoto, H. Kurata, R. Kishi, Y. Shigeta, M. Nakano, K. Tokunaga, K. Kamada, T. Kubo, *J. Am. Chem. Soc.* **2013**, *135*, 1430–1437.
- [15] Y. Tian, K. Uchida, H. Kurata, Y. Hirao, T. Nishiuchi, T. Kubo, *J. Am. Chem. Soc.* **2014**, *136*, 12784–12793.

Received: August 2, 2015

Published online on November 12, 2015